Demonstration of a Direct Interaction between σ-1 Receptors and Acid-Sensing Ion Channels

Stewart M. Carnally,[†] Molly Johannessen,[‡] Robert M. Henderson,[†] Meyer B. Jackson,[‡] and J. Michael Edwardson[†*]

[†]Department of Pharmacology, University of Cambridge, Cambridge, United Kingdom; and [‡]Department of Physiology, University of Wisconsin, Madison, Wisconsin

ABSTRACT The σ-1 receptor is a widely expressed protein that interacts with a variety of ion channels, including the acid-sensing ion channel (ASIC) 1a. Here we used atomic force microscopy to determine the architecture of the ASIC1a/σ-1 receptor complex. When isolated His_8-tagged ASIC1a was imaged in complex with anti-His_6 antibodies, the angle between pairs of bound antibodies was 135°, consistent with the known trimeric structure of the channel. When ASIC1a was coexpressed with FLAG/His_6-tagged σ-1 receptor, ASIC1a became decorated with small particles, and pairs of these particles bound at an angle of 131°. When these complexes were incubated with anti-FLAG antibodies, pairs of antibodies bound at an angle of 134°, confirming that the small particles were σ-1 receptors. Of interest, we found that the σ-1 receptor ligand haloperidol caused an ~50% reduction in ASIC1a/σ-receptor binding, suggesting a way in which σ-1 ligands might modulate channel properties. For the first time, to our knowledge, we have resolved the structure of a complex between the σ-1 receptor and a target ion channel, and demonstrated that the stoichiometry of the interaction is 1 σ-1 receptor/1 ASIC1a subunit.

INTRODUCTION

The σ-receptor was initially believed to be a type of opioid receptor (1); however, it is now clear that it is a distinct receptor consisting of two subtypes: σ-1 and σ-2 (reviewed in Monnet (2)). The σ-1 receptor has been cloned (3) and shown to share 30% identity and 67% similarity with a yeast sterol C8-C7 isomerase (ERG2). The receptor contains two transmembrane regions, although it is still unclear whether the N- and C-termini are cytoplasmic (4) or extracytoplasmic (5). The sequence of the σ-2 receptor is still unknown. The σ-1 receptor is widely expressed in both the central nervous system and peripheral tissues (2), and a variety of functions have been ascribed to it, including modulation of voltage-gated K^+ (4,6–8), Na^+ (9), and Ca^{2+} (10) ion channel activity at the plasma membrane; control of Ca^{2+} release from the endoplasmic reticulum (5); and neuroprotection in cerebral ischemia and stroke (11). Further, there is a genetic linkage with schizophrenia (12).

σ-1 Receptors are activated by a wide variety of ligands (reviewed in Monnet (2)), including antipsychotic drugs (e.g., haloperidol), and psychotomimetics (e.g., pentazocine), and it was recently shown that the hallucinogen *N*,*N*-dimethyltryptamine is an endogenous ligand at this receptor (13). Mutational analysis has identified residues D126 and E172 in the C-terminus as being crucial to ligand binding (14). In addition, two so-called sterol binding-like domains have been identified (15,16). One of these domains (residues 91–109) encompasses part of the second transmembrane domain, and the other (residues 176–194) forms a hydrophobic region close to the C-terminus. The C-terminal hydrophobic region contains cholesterol-binding domain motifs (VEYGR and LFYTLRSYAR), and, as expected, this region binds cholesterol (17). Significantly, cholesterol binding is strongly inhibited by the classical σ-1 receptor ligand SKF10047, suggesting that the cholesterol-binding domain forms part of the drug-binding site (17).

Modulation of the voltage-gated K^+ channel by the σ-1 receptor does not involve transduction mechanisms such as G-protein signaling or phosphorylation (18), suggesting that a direct interaction between the two proteins is required. In support of this idea, Kv1.4 and the σ-1 receptor can be coimmunoprecipitated from membrane lysates prepared from both rat posterior pituitary cells and mRNA-injected *Xenopus* oocytes (4).

The properties of acid-sensing ion channels (ASICs) are also modulated by σ-1 receptors (19). ASICs belong to the degenerin/epithelial Na^+ channel family of cation channels (reviewed in Wemmie et al. (20)). They are activated by extracellular protons and are selectively permeable to Na^+ ions. They are found in all vertebrates examined thus far, and are responsible for acid-evoked currents in many neurons of the peripheral and central nervous systems. They appear to play diverse roles in functions such as nociception, learning, and memory, and in pathological conditions such as ischemic stroke. Each ASIC subunit spans the membrane twice, and the N- and C-termini are intracellular (20). The stoichiometry of the complete ASIC has been controversial; however, the recent determination of the crystal structure of ASIC1a showed that the channel is a trimer (21). This trimeric structure has been confirmed by atomic force microscopy (AFM) imaging of the intact channel (22).

Submitted October 5, 2009, and accepted for publication December 15, 2009.

*Correspondence: jme1000@cam.ac.uk

Editor: Hassane Mchaourab.

0006-3495/10/04/1182/10 $2.00

doi: 10.1016/j.bpj.2009.12.4293

There are four ASIC genes, which produce six subunit isoforms: ASIC1a, ASIC1b, ASIC2a, ASIC2b, ASIC3, and ASIC4 (20). These subunits assemble to form both homo- and heteromultimers with varying properties, including differential sensitivity to pH (23), and Ca^{2+} permeabilities (for example, ASIC1a homomers are Ca^{2+} permeable, whereas ASIC1a/ASIC2 heteromers are not (24)). It was recently shown (19) that stimulation of the σ-1 receptor endogenously expressed in rat cortical neurons inhibits ASIC1a-mediated membrane currents and reduces consequent intracellular Ca^{2+} accumulation, suggesting that σ-1 receptors may represent a therapeutic target for improving the outcome of stroke injury. What is not clear from these experiments is whether the interaction between the σ-1 receptor and ASIC1a is direct, and, if so, what the ASIC1a/σ-1 receptor complex looks like.

We have developed a method, based on AFM imaging, for directly determining the arrangement of subunits within multimeric proteins. The method involves the imaging of isolated proteins and of complexes formed between the proteins and subunit-specific antibodies. We have applied this method to the architecture of the P2X receptor (25), the 5-HT_3 receptor (26), the $GABA_A$ receptor (27), the transient receptor potential C1 ion channel (28), and ASIC1a (22). In the study presented here, we used AFM imaging to address the nature of the interaction between the σ-1 receptor and ASIC1a. For the first time, to our knowledge, we demonstrate the structure of an ion channel/σ-1 receptor complex and show that the stoichiometry of this complex is 1 receptor/1 channel subunit.

MATERIALS AND METHODS

Cell culture

HEK-293 cells, stably transfected with human ASIC1a bearing a C-terminal His_8 tag, were grown in Dulbecco's modified Eagle's medium supplemented with 10% (v/v) newborn calf serum, 100 units/mL penicillin, 100 mg/mL streptomycin, and 100 mg/mL Zeocin (Invitrogen, Paisley, UK) in an atmosphere of 5% CO_2/air. tsA201 cells, a subclone of HEK-293 cells stably expressing the SV40 large T-antigen, were grown under the same conditions but without Zeocin and with 10% (v/v) fetal bovine serum instead of newborn calf serum.

σ-1 Receptor construct

A cDNA sequence encoding the human σ-1 receptor, with a C-terminal FLAG epitope, was subcloned into the vector pcDNA3.1/V5-His using *Hin*dIII and *Age*I so as to delete the V5 epitope tag but leave the His_6 tag. The sequence of the construct was verified before use.

Transient transfection of HEK-293 cells and tsA201 cells

Transfection of cells was carried out with the use of a CalPhos mammalian transfection kit (Clontech, Basingstroke, UK). After transfection, the cells were incubated for 48 h at 37°C to allow expression of the receptors. Protein expression and intracellular localization were checked by immunofluorescence analysis of small-scale cultures. Cells were fixed, permeabilized, and incubated with appropriate primary antibodies, followed by fluorophore-conjugated goat anti-mouse or anti-rabbit secondary antibodies (Sigma, Poole, UK). The cells were then imaged by confocal laser scanning microscopy.

Solubilization and purification of $His_{8/6}$-tagged proteins

Solubilization and purification were performed as described previously (25). Briefly, a crude membrane fraction prepared from the cells was solubilized in 1% (w/v) 3-[(3-cholamidopropyl)dimethylammonio]-1-propanesulfonate (CHAPS), and the solubilized material was incubated with Ni^{2+}-agarose beads (Probond; Invitrogen). The beads were washed extensively and bound proteins were eluted with increasing concentrations of imidazole. Samples were analyzed by sodium dodecyl sulfate polyacrylamide gel electrophoresis (SDS-PAGE). Proteins were detected by silver staining or immunoblotting using rabbit polyclonal antibodies against either ASIC1a (Alomone, Buckingham, UK) or the human σ-1 receptor (Abcam, Cambridge, UK), and a mouse monoclonal antibody against the FLAG tag on the σ-1 receptor (Sigma).

AFM imaging

ASICs, anti-His_6 antibodies, and σ-1 receptors were initially imaged alone. ASICs were then imaged after an overnight incubation at 4°C with a 1:2 molar ratio (~0.2 nM ASIC concentration) of anti-His_6 monoclonal antibody (Invitrogen). An anti-FLAG antibody was used as a negative control. ASIC/σ-1 receptor complexes were imaged either alone or after incubation with anti-FLAG antibody. An anti-V5 antibody (Invitrogen) was used as a negative control. Proteins were diluted to a final concentration of 0.04 nM, and 45 μL of the sample were allowed to adsorb to freshly cleaved, poly-L-lysine-coated mica disks. After a 10-min incubation, the samples were washed with BPC-grade water (Sigma) and dried under nitrogen. Imaging was performed with a Veeco Digital Instruments multimode atomic force microscope controlled by a Nanoscope IIIa controller. The samples were imaged in air, using tapping mode. The silicon cantilevers used had a resonant frequency of ~300 kHz and a specified spring constant of 40 N/m (Olympus). The applied imaging force was kept as low as possible ($A_s/A_0 \sim 0.85$).

The molecular volumes of the protein particles were determined from particle dimensions based on AFM images. After adsorption of the channels onto the mica support, the particles adopted the shape of a spherical cap. The heights and radii were measured from multiple cross sections of the same particle, and the molecular volume was calculated using the following equation:

$$V_m = (\pi h/6)\left(3r^2 + h^2\right), \quad (1)$$

where h is the particle height and r is the radius (25). Volumes were initially calculated using an automated program that we developed in-house (29). The output of the program was then checked manually to exclude false-negatives and false-positives.

Molecular volume based on molecular mass was calculated using the following equation:

$$V_c = (M_0/N_0)(V_1 + dV_2), \quad (2)$$

where M_0 is the molecular mass; N_0 is Avogadro's number; V_1 and V_2 are the partial specific volumes of particle and water, respectively; and d is the extent of protein hydration (taken as 0.4 g water/g protein). Because the ASIC1a subunits are glycoproteins, the volume contributions of core protein and attached oligosaccharides were calculated separately, using values of partial specific volumes for protein (0.74 cm^3/g) and carbohydrate (0.61 cm^3/g), as described previously (22). We assumed a subunit protein molecular mass of 60 kDa and an additional contribution from oligosaccharides of 10 kDa.

Determination of the association of proteins with rafts

Cells were extracted in ice-cold Triton X-100 (1%) and the extracts were mixed with Optiprep (Sigma) to a concentration of 35% (v/v). Increasingly dilute solutions of Optiprep were layered above the cell extracts and the discontinuous density gradients (total volume 9 mL) were centrifuged at 200,000 *g* for 4 h. Samples (1 mL) were taken from the tops of the gradients, and proteins (ASIC1a, σ-1 receptor and the raft marker caveolin) in the fractions were analyzed by SDS-PAGE and immunoblotting. Caveolin was detected using a rabbit polyclonal antibody (Sigma).

RESULTS

Immunofluorescence analysis of HEK-293 cells stably expressing ASIC1a bearing a His_8 epitope tag at its C-terminus, using either anti-ASIC1a or anti-His_6 antibodies, revealed the presence of ASIC1a channels in the transfected cells (Fig. 1 *A*). The staining pattern indicated that the channels were present both at the plasma membrane and in internal membranes. In contrast, the use of an anti-V5 antibody as a negative control produced only a background immunofluorescence signal (data not shown). When the cells were transfected with a FLAG/His_6-tagged σ-1 receptor construct, immunofluorescence with anti-FLAG antibodies showed the presence of σ-1 receptors in ~20% of the cells (compare the fluorescence image with the corresponding brightfield image in Fig. 1 *B*).

A crude membrane fraction prepared from the ASIC1a-expressing cells was solubilized in CHAPS detergent (1% w/v), and ASICs were isolated through the binding of the His_8 tag to Ni^{2+}-agarose beads. Both the membrane fraction and the isolated protein were subjected to SDS-PAGE, silver staining, and immunoblotting using the anti-ASIC1a antibody. A silver stain of the isolated fraction (Fig. 1 *C*, *left panel*) showed a single band at a molecular mass of 70 kDa, consistent with the expected size of the ASIC1a subunit (30). The anti-ASIC1a antibody also labeled a single band, again at a molecular mass of 70 kDa (Fig. 1 *C*, *right panel*). Hence, the isolation procedure produced highly purified ASIC1a.

When proteins were isolated from crude membrane fractions of cells transfected with FLAG/His_6-tagged σ-1 receptor and subjected to SDS-PAGE followed by silver staining and immunoblotting, prominent bands were seen on the silver-stained gel at molecular masses of 70 kDa and 33 kDa, as expected from the known sizes of ASIC1a (29) and the σ-1 receptor with added FLAG and His_6 tags (3) (Fig. 1 *D*, *left panel*). Other bands were visible, although the 70-kDa and 33-kDa bands were the most prominent. Immunoblotting (Fig. 1 *D*, *right panels*) confirmed that the 70-kDa protein was ASIC1a and the 33-kDa protein was FLAG-tagged σ-1 receptor. It is known that HEK-293 cells endogenously express the σ-1 receptor (9). To assess the relative expression levels of endogenous and exogenous (FLAG/His_6-tagged)

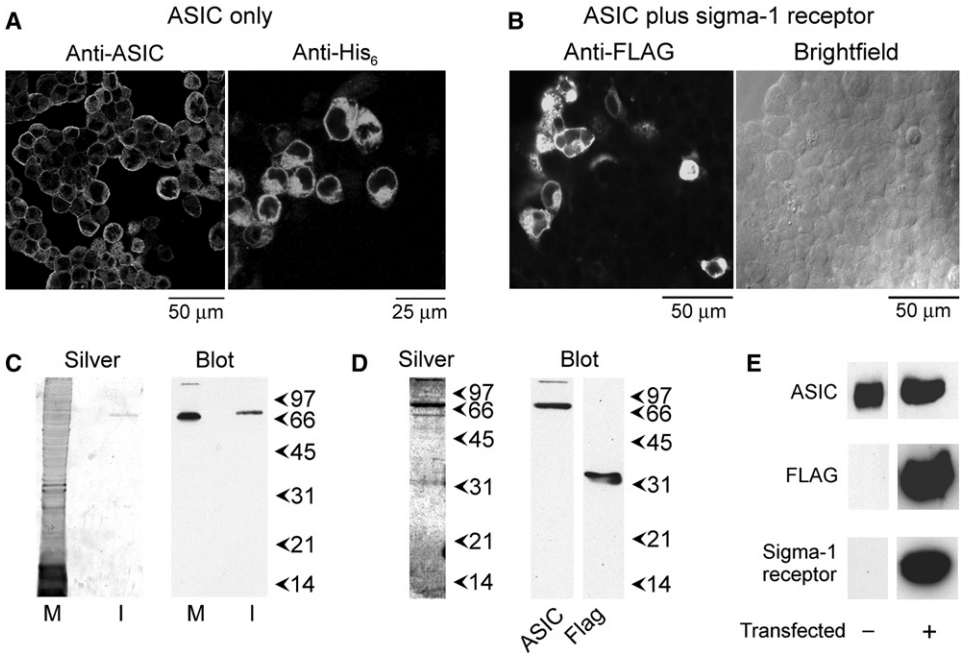

FIGURE 1 Isolation of proteins from ASIC1a-expressing cells. (*A*) Immunofluorescence detection of ASIC1a in stably transfected HEK-293 cells. Cells were fixed, permeabilized, and incubated with either rabbit polyclonal anti-ASIC1a antibody or mouse monoclonal anti-His_6 antibody, followed by Cy3-conjugated goat anti-rabbit or anti-mouse secondary antibodies, as appropriate. Cells were imaged by confocal laser scanning microscopy. (*B*) Immunofluorescence detection of the σ-1 receptor in HEK-293 cells stably expressing ASIC1a and transiently transfected with σ-1 receptor cDNA. Cells were incubated with mouse monoclonal anti-FLAG antibody, followed by fluorescein isothiocynate-conjugated goat anti-mouse secondary antibodies. A representative immunofluorescence image is shown, along with a corresponding brightfield image; ~20% of the cells are expressing the σ-1 receptor. (*C*) Detection of ASIC1a in a membrane fraction from stably transfected cells (M) and after isolation (I) by binding to Ni^{2+}-agarose. Samples were analyzed by SDS-PAGE and either silver staining (*left panel*) or immunoblotting (*right panel*) using rabbit polyclonal anti-ASIC1a antibody, followed by a horseradish peroxidase-conjugated goat anti-rabbit secondary antibody. Immunoreactive bands were visualized using enhanced chemiluminescence. Arrowheads indicate molecular mass markers (kDa). (*D*) Detection of ASIC1a and the σ-1 receptor after isolation from σ-1 receptor-transfected cells by binding to Ni^{2+}-agarose. Samples were analyzed by SDS-PAGE and either silver staining (*left panel*) or immunoblotting (*right panel*) using anti-ASIC1a antibody or mouse monoclonal anti-FLAG antibody. (*E*) A screen for the presence of endogenous σ-1 receptor in protein samples isolated from nontransfected ASIC1a-expressing cells or σ-1 receptor-transfected cells. Samples were analyzed by SDS-PAGE and immunoblotting using anti-ASIC1a antibody, anti-FLAG antibody, or rabbit polyclonal anti-σ-1 receptor antibody.

receptors, we subjected isolated protein fractions prepared from cells expressing either ASIC1a alone or ASIC1a plus FLAG/His_6-tagged σ-1 receptor to immunoblot analysis (Fig. 1 *E*). As expected, both samples gave a strong signal with an anti-ASIC1a antibody. The cells transfected with FLAG/His_6-tagged receptors also gave strong signals with both an anti-FLAG antibody and an anti-σ-1 receptor antibody. In contrast, the nontransfected cells gave no detectable signal with either the anti-FLAG antibody (as expected) or, significantly, with the anti-σ-1 receptor antibody. Hence, the endogenous σ-1 receptors must be expressed at much lower levels than the FLAG/His_6-tagged receptors, and are therefore unlikely to interfere with the subsequent analysis of ASIC1a/σ-1 receptor interaction.

Isolated ASIC1a, anti-His_6 antibodies, and σ-1 receptors (prepared in the absence of ASIC1a by transfection of tsA201 cells) were subjected to AFM imaging. In previous work, we used AFM probes made of silicon nitride. To measure molecular volumes, we assumed that the shape the particles adopted the approximate shape of a spherical cap. To overcome the large tip-convolution effect, we measured the particle radius at half-height. Using this procedure, we determined a volume of 210 nm^3 for the ASIC1a trimer, which is considerably smaller than the expected value of 390 nm^3 (22). Nevertheless, the trimeric structure of the channel was apparent from the presence of the triple subunit clusters, likely caused by ASIC1a trimers attaching to the mica substrate intact and then falling apart during the drying process. More recently, we have begun to use probes made of silicon, which have a higher aspect ratio and a much greater spring constant than the silicon nitride tips. With the new tips, we have found that we can achieve a more accurate estimation of the protein volume using the basal radius rather than the half-height radius in Eq. 1. We have demonstrated this by imaging a range of proteins of known molecular mass and comparing the measured volumes with the expected volumes (31). Of course, even the new probes will inevitably display some lateral broadening, so there will be some overestimation of molecular volumes. However, this effect will likely be mitigated by the reduction in the measured vertical dimension resulting from increased squashing of the particles, because of the higher spring constant of the probes.

A low-magnification image of isolated ASICs is shown in Fig. 2 *A*. A mixed population of particles is seen, including a number of large particles, two of which are numbered. The

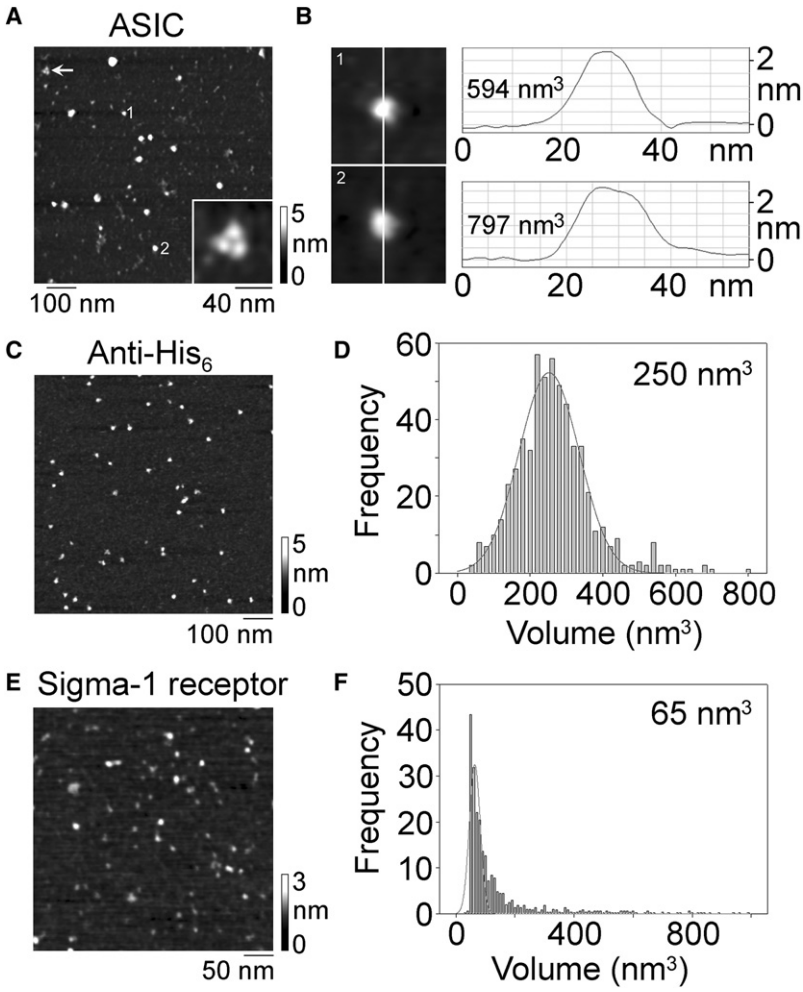

FIGURE 2 AFM imaging of ASIC1a, anti-His_6 antibodies, and σ-1 receptors. (*A*) Low-magnification image of isolated ASIC1a. The arrow indicates a trimeric cluster of three equally sized particles, which is likely an ASIC trimer that has bound to the mica intact and then fallen apart during the drying process. A zoomed image of this cluster is shown at the bottom right of the panel. A shade-height scale is shown at the right. (*B*) Sections through the two particles indicated in *A*, taken at the positions indicated by the lines. The sections indicate that the shapes of the particles approximate that of a spherical cap. The calculated volumes of the particles are indicated. (*C*) Low-magnification image of anti-His_6 antibodies. A shade-height scale is shown at the right. (*D*) Frequency distribution of molecular volumes of anti-His_6 antibodies. The curve indicates the fitted Gaussian function. The mean of the distribution is indicated. (*E*) Low-magnification image of σ-1 receptors. A shade-height scale is shown at the right. (*F*) Frequency distribution of molecular volumes of σ-1 receptors. The curve indicates the fitted Gaussian function. The mean of the distribution is indicated.

arrow indicates a characteristic triple subunit cluster (referred to above), and a zoomed image of this cluster is shown in the inset. Sections through particles 1 and 2 show that they adopt the approximate shape of a spherical cap (Fig. 2 *B*). Using Eq. 1, the volumes of the particles were calculated as 594 and 737 nm^3, respectively. These values are considerably higher than the expected value of 390 nm^3 for an ASIC1a trimer, and may indicate the presence of attached detergent, as we have suggested previously for other multispanning transmembrane proteins (25–27). Fig. 2 *C* shows a low-magnification image of anti-His_6 antibodies. A frequency distribution of molecular volumes (Fig. 2 *D*) gave a mean molecular volume of 250 nm^3, close to the volume of 285 nm^3 expected for a 150-kDa immunoglobulin G molecule. Isolated σ-1 receptor particles appeared as a spread of small particles (Fig. 2 *E*), and the frequency distribution of molecular volumes gave a mean molecular volume of 65 nm^3, very close to the value of 63 nm^3 expected for a 33-kDa FLAG/His_6-tagged σ-1 receptor.

For the reasons described above, the measured volume is not by itself a reliable indicator of the stoichiometry of the ASIC1a channel. To conclusively establish the stoichiometry of the channels, they were imaged after antibody decoration. ASIC1a complexes isolated from ASIC1a-expressing cells were incubated with an anti-His_6 antibody, which should decorate the C-terminal His_8 epitope tag present on each subunit. Three low-magnification AFM images of ASIC1a-antibody complexes are shown in Fig. 3 *A*. Several large particles can be seen, some of which have been decorated by either one (*arrowheads*) or two (*arrows*) smaller particles. A gallery of undecorated and singly or doubly decorated large particles is shown in Fig. 3 *B*. Of the large particles imaged, 88.7% were undecorated, 9.8% were singly decorated, and 1.5% were doubly decorated. We presumed that the large particles represented ASICs and the smaller particles represented antibodies.

The molecular volumes of the doubly decorated central particles ($n = 50$) and the corresponding peripheral particles

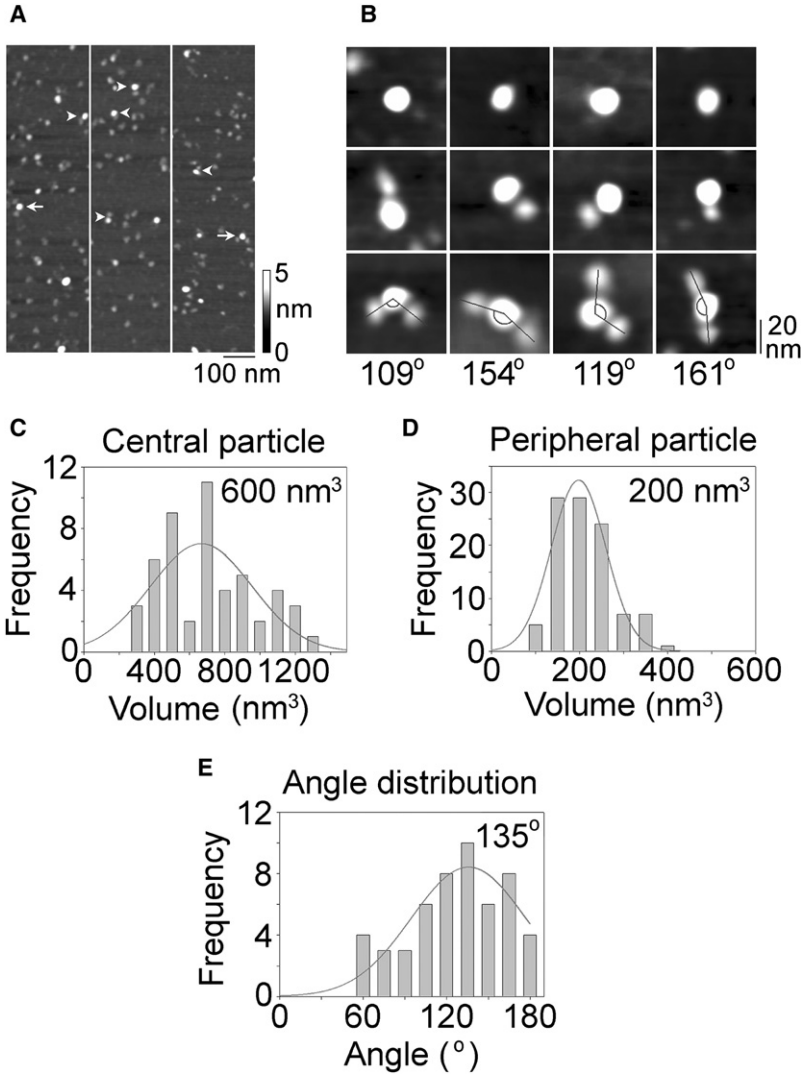

FIGURE 3 Analysis of anti-His_6 antibody binding to His_8-tagged ASIC1a. (*A*) Low-magnification AFM images of a sample of isolated ASIC1a that had been incubated with anti-His_6 antibody. Arrowheads indicate singly decorated ASICs; arrows indicate doubly decorated ASICs. A shade-height scale is shown at the right. (*B*) Gallery of zoomed images of ASICs that are undecorated (*top*) or decorated by one (*middle*) or two (*bottom*) anti-His_6 antibodies. Lines indicate the angles between pairs of bound antibodies. (*C–E*) Frequency distributions of (*C*) molecular volumes of decorated central particles, (*D*) molecular volumes of bound peripheral particles, and (*E*) angles between pairs of bound peripheral particles. The curves indicate the fitted Gaussian functions. The means of the distributions are indicated.

were determined and used to construct frequency distributions. The mean volume of the central particles was 600 nm^3 (Fig. 3 *C*), similar to the volumes of the large particles seen in the images of isolated ASICs (Fig. 2, *A* and *B*). The mean volume of the peripheral particles was 200 nm^3 (Fig. 3 *D*), a little smaller than the volume determined for isolated anti-His_6 antibodies (Fig. 2, *C* and *D*). This apparent volume slippage from the small peripheral particles to the large central particles is a common feature of this type of experiment (see below) and is likely caused by the different extents of spreading of the two types of particle on the mica substrate (i.e., the large particle spreads out more and partially engulfs the smaller particles). In addition to this problem of volume slippage, measurement of molecular volumes is further complicated by the convolution introduced by the geometry of the scanning tip, as explained above. Hence, the measured volume is not by itself a reliable indicator of the stoichiometry of the channel.

To conclusively establish the stoichiometry of the channel, we identified doubly decorated ASICs and measured the angles between the bound antibodies. This was done in each case by joining the highest point on the central particle (the ASIC trimer) to the highest points on the peripheral particles (the antibodies) by lines and then determining the angle between the two lines. The frequency distribution of angles obtained is shown in Fig. 3 *E*. The mean angle is 135°, close to the expected value of 120° for a trimeric ASIC. The antibody decoration profile, then, strongly indicates that ASIC1a assembles as a trimer. In a control experiment, we incubated the isolated ASICs with anti-FLAG antibodies. Now only 0.2% of the large particles were doubly decorated, compared with the value of 1.5% obtained with the anti-His_6 antibody. These double-decoration events in the control incubation likely represent occasions when the antibodies attached to the mica close enough to the ASIC particles to give the appearance of direct binding. These data support our conclusion that the isolated ASICs were being specifically decorated by the anti-His_6 antibodies.

When the proteins isolated from ASIC1a/σ-1 receptor expressing cells were imaged by AFM, a spread of large particles, some of which had one or two small particles attached, was observed. Note that the protein fraction likely contained free σ-1 receptor particles, since the σ-1 construct bears a His_6 epitope tag. However, these particles would be difficult to distinguish from ASIC1a monomers, which would also have been present, as observed in a previous study (22). A gallery of undecorated and singly or doubly decorated large particles is shown in Fig. 4 *A*. Of the large particles imaged, 87.3% were undecorated, 11.4% were singly decorated by small particles, and 1.3% were doubly decorated. A frequency distribution of molecular volumes of the central particles in these complexes (Fig. 4 *B*) gave a mean volume of 550 nm^3, similar to the volume illustrated in Figs. 2 and 3. The frequency distribution of molecular volumes of the small particles (Fig. 4 *C*) gave a mean volume of 50 nm^3, smaller than the volume of 65 nm^3 determined for isolated σ-1 receptors (Fig. 2, *E* and *F*). Hence, volume slippage between the small and large particles is again apparent. We conclude that the central particles again represent ASICs, whereas the peripheral particles represent bound σ-1 receptors. The angle distribution for pairs of bound σ-1 receptors is shown in Fig. 4 *D*. The mean angle is 131°, very close to the value for double decoration of the ASIC1a by anti-His_6 antibodies, and also to the expected value of 120° for a trimeric channel structure. This result suggests that the σ-1 receptors bind with a stoichiometry of 1 σ-1 receptor/1 ASIC1a subunit.

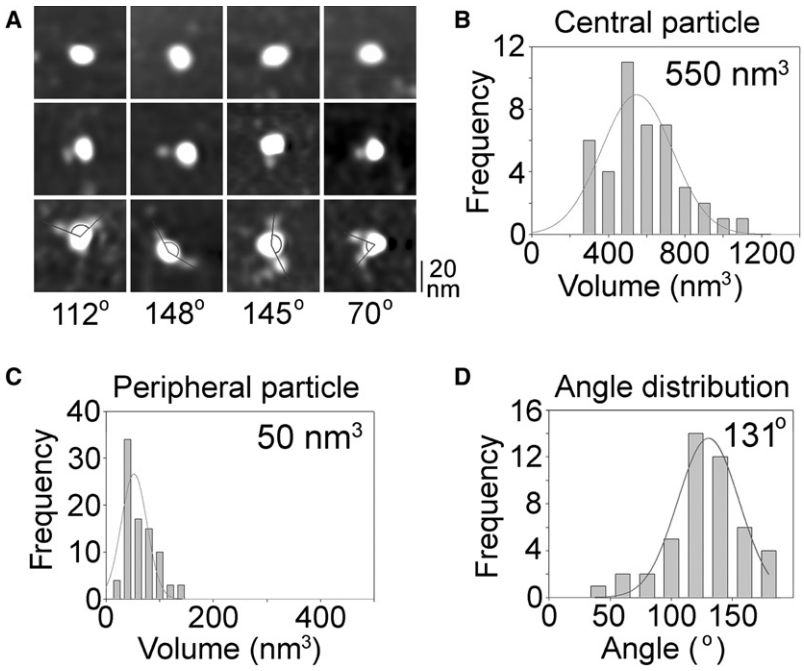

FIGURE 4 Analysis of σ-1 receptor binding to ASIC1a. (*A*) Gallery of zoomed images of ASICs that are undecorated (*top*) or decorated by one (*middle*) or two (*bottom*) peripheral particles. Lines indicate the angles between pairs of bound peripheral particles. (*B–D*) Frequency distributions of (*B*) molecular volumes of decorated central particles, (*C*) molecular volumes of bound peripheral particles, and (*D*) angles between pairs of bound peripheral particles. The curves indicate the fitted Gaussian functions. The means of the distributions are indicated.

To confirm that the small particles seen decorating the ASICs are indeed σ-1 receptors, we incubated the proteins isolated from the ASIC1a/σ-1 receptor-expressing cells with anti-FLAG antibodies. We have shown (above) that these antibodies do not decorate ASICs alone; however, they ought to decorate σ-1 receptors complexed with the ASICs. Now, large central particles (ASICs) could be seen decorated with one or two peripheral particles, many of which were larger than those seen in the absence of the antibody. Of the peripheral particles observed, 55% of the total were large and therefore likely to be antibodies bound to σ-1 receptors, whereas 45% were small and therefore likely to be undecorated σ-1 receptors. A gallery of images showing undecorated ASICs and ASICs decorated with either one or two large peripheral particles is shown in Fig. 5 *A*. Of the ASIC1a particles imaged, 87.1% were undecorated, 6.6% were singly decorated, and 1.2% were doubly decorated by larger peripheral particles. A molecular volume distribution for the large peripheral particles is shown in Fig. 5 *B*. The mean molecular volume of these particles is 210 nm^3, slightly larger than the volume reported above for the anti-His_6 antibody (Fig. 2 *D*), consistent with the combined contributions of a σ-1 receptor and an antibody. The angle distribution for pairs of bound peripheral particles is shown in Fig. 5 *C*. The mean angle is 134°, very close to the value of 131° for the double decoration of ASICs by the smaller peripheral particles in the previous experiment. When an anti-V5 antibody was used instead of the anti-FLAG antibody, only a very low level (0.2%) of decoration of the central particles with two larger peripheral particles was seen. We therefore conclude that these particles represent anti-FLAG antibodies bound to the FLAG/His_6-tagged σ-1 receptors, which are in turn complexed with the ASICs.

Since ligands acting at σ-1 receptors are known to affect ion channel function, we tested the effect of one of these ligands, haloperidol, on the interaction between the σ-1 receptor and ASIC1a. ASIC1a-expressing cells were transfected with cDNA for the σ-1 receptor and proteins were isolated in the normal way, by binding to Ni^{2+}-agarose. In this case, however, haloperidol (10 μM) was added to the culture medium 48 h before cell lysis, and the drug was present at the same concentration throughout the protein isolation. Immunoblotting of crude cell extracts showed that preincubation of the cells with haloperidol did not change the expression level of the σ-1 receptor (data not shown). Hence, haloperidol did not cause any down-regulation of the σ-1 receptor. Isolated proteins were subjected to AFM imaging as above, and the numbers of ASIC1a particles decorated by peripheral σ-1 receptor particles were determined. It was found that haloperidol caused a reduction in single decoration events from 11.4% to 6.0%, and a reduction in double decoration from 1.3% to 0.8%. Given that the reduction in single binding events is ~50%, we would actually expect a >50% reduction in double binding. However, since the proportion of double binding events is so low, and there is also some

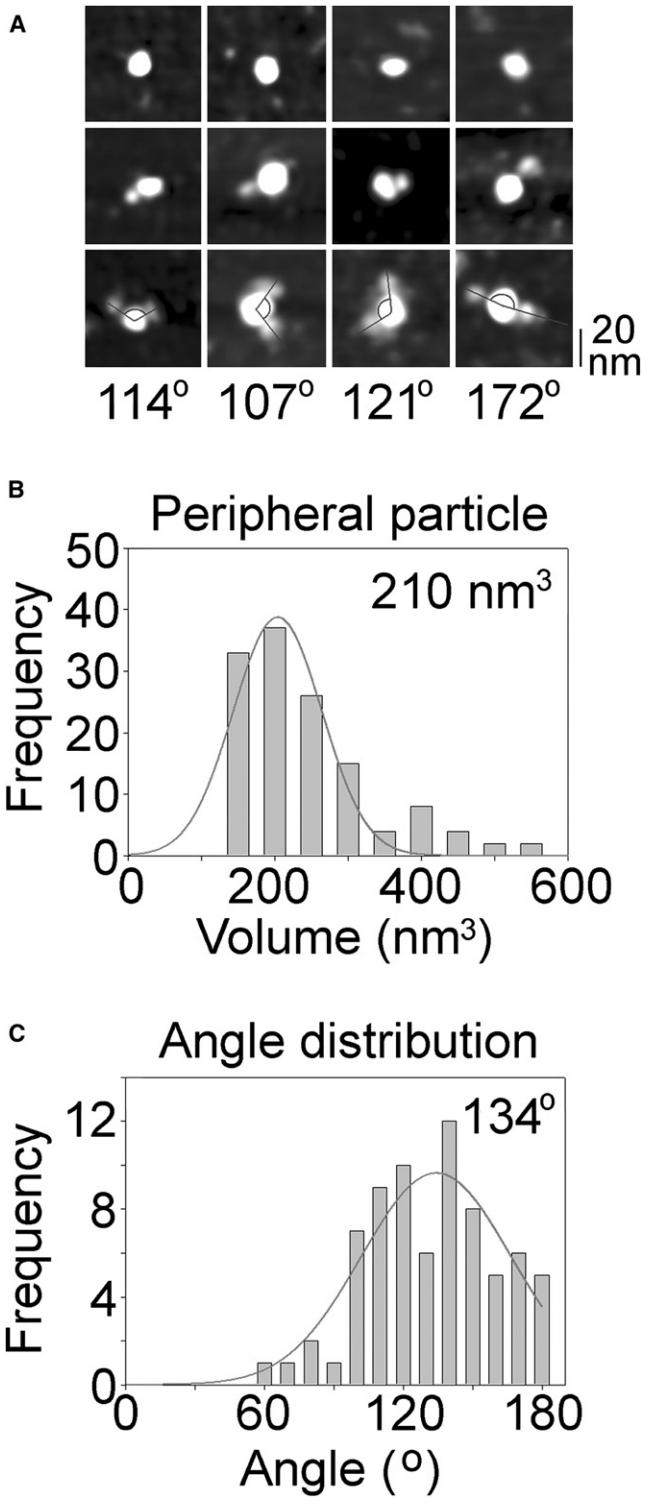

FIGURE 5 Decoration of bound σ-1 receptors with anti-FLAG antibodies. (*A*) Gallery of zoomed images of ASICs/σ-1 receptor complexes that are undecorated (*top*) or decorated by one (*middle*) or two (*bottom*) peripheral particles. Lines indicate the angles between pairs of bound large peripheral particles. (*B*) Frequency distribution of molecular volumes of bound peripheral particles. The curve indicates the fitted Gaussian function. The mean of the distribution is indicated. (*C*) Frequency distribution of angles between pairs of bound peripheral particles. The curve indicates the fitted Gaussian function. The mean of the distribution is indicated.

degree of nonspecific decoration, we believe it would be unwise to overanalyze these data.

It has been reported that treatment of cells with the σ-1 receptor ligand SKF10047 reduces the proportion of the σ-1 receptor in lipid raft fractions of the plasma membrane (17). Drug treatment also reduced the cholesterol content of rafts, and the raft targeting of other known raft marker proteins, such as flotillin. These results suggest that the σ-1 receptor may be able to sequester cholesterol into membranes, potentially remodeling lipid rafts. Since at least some of the targets of σ-1 receptors, such as Kv1.4 and Kv1.5, are known raft residents (32,33), and cholesterol depletion significantly affects the kinetic properties of these channels, it is possible that the effects of σ-1 receptor drugs may be caused by a remodeling of raft lipid content.

The ability of σ-1 receptor ligands to displace cholesterol from its binding site on the receptor may be relevant to the observed reduction in ASIC1a/σ-1 receptor coupling caused by haloperidol in this study. We hypothesized that the functional effect of the σ-1 receptor on ASIC1a might be brought about by the recruitment of ASIC1a into lipid rafts. By reducing the ASIC1a/σ-1 receptor coupling, haloperidol might reduce this putative raft recruitment of ASIC1a. We explored this idea by determining the effect of the σ-1 receptor (with and without haloperidol) on the partitioning of ASIC1a between raft and non-raft phases. Cells were extracted in ice-cold Triton X-100, and the extracts were subjected to density gradient centrifugation. It is known that rafts resist solubilization and thus float in gradients (34). As shown in Fig. 6, ASIC1a was found predominantly in the lower (denser) fractions of the gradient under all three conditions tested (ASIC1a only, ASIC1a plus σ-1 receptor, and ASIC1a plus σ-1 receptor plus haloperidol). Hence, the vast majority of ASIC1a was not raft-associated, and its partitioning between raft and non-raft phases was not affected by either the σ-1 receptor or haloperidol. Fig. 5 also shows that the σ-1 receptor itself was also predominantly excluded from rafts. In contrast, the raft marker, caveolin, floated toward the top of the gradient, as expected, and this behavior was not affected by the presence of the σ-1 receptor.

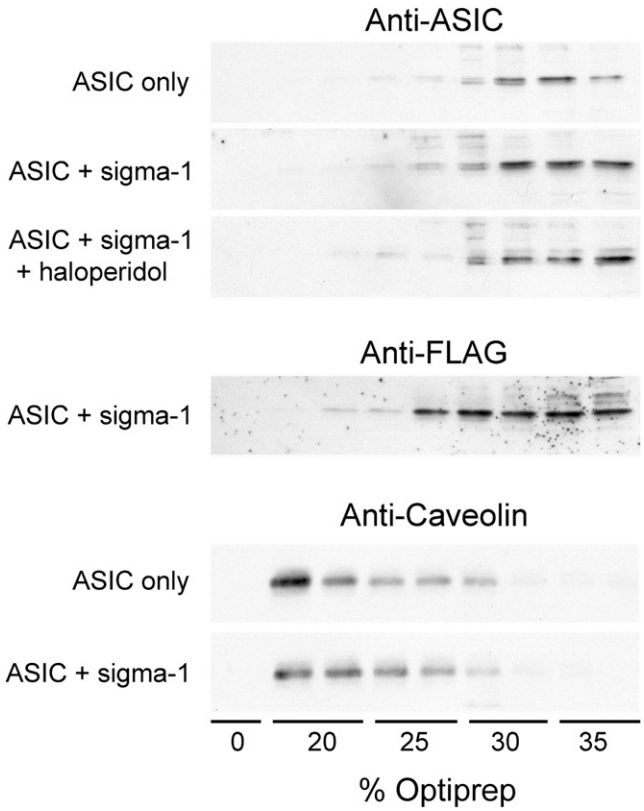

FIGURE 6 Determination of the raft association of ASIC1a and the σ-1 receptor. Cells were extracted with ice-cold Triton X-100 (1%) and subjected to centrifugation on Optiprep density gradients. Fractions from the gradient were analyzed by SDS-PAGE and immunoblotting using anti-ASIC1a antibody, anti-FLAG antibody (for the σ-1 receptor), or anti-caveolin antibody (as a raft marker).

DISCUSSION

σ-1 Receptor ligands have been shown to inhibit many different ion channels, including ASICs (19), and a number of voltage-gated channels (4–9). The ability of σ-1 receptors to modulate ion channel activity does not require G-protein activation or protein phosphorylation (18), suggesting that there is a direct interaction between the σ-1 receptor and its target channels. The ability of the σ-1 receptor to alter the function of Kv1.4 channels in the absence of ligand (4) is consistent with this suggestion. The observed coimmunoprecipitation of the two proteins, even in a heterologous system, also indicates a direct interaction (4), although these findings do not rule out the involvement of another adaptor molecule.

In this study, we used AFM imaging to visualize ASIC1a isolated from cells that stably express this protein. The trimeric structure of the ASIC is now well established as a result of the recent publication of the crystal structure (21). In a previous AFM study (22), we detected a mixture of ASIC1a subunit monomers, dimers, and trimers, and in some cases triple-subunit clusters were clearly visible, confirming the trimeric structure of the channel. Here, we show that antibody decoration of isolated His_8-tagged ASIC1a complexes reflects this trimeric structure, in that the mean angle between pairs of bound anti-His_6 antibodies is close to the expected value of 120°. The trimeric structure of the intact ASIC1a channel cannot be discerned directly in the AFM images, largely as a result of the collapse of the receptors onto the mica substrate. We have considered the possibility that imaging under fluid might improve the quality of our images. However, the collapse of the particles onto the mica does not depend primarily on the medium (i.e., air or fluid). In fact, in a previous study, various proteins were imaged under fluid as well as in air, and although the measured volumes were similar in the two cases, no

additional structural features became apparent during fluid imaging (35). In addition, if we were to image under fluid, the particles would appear wider because fluid-imaging tips are blunter than air-imaging tips. This reduction in lateral resolution would make it difficult to resolve bound antibodies, and especially bound σ-1 receptors, as distinct particles. For these reasons, we used imaging in air for the study presented here.

When ASIC-expressing cells were transiently transfected with cDNA encoding σ-1 receptors, some of the isolated ASICs were decorated by smaller particles. The mean molecular volume of these particles was similar to the expected size of the σ-1 receptor; the particles were not seen when ASICs were isolated from untransfected cells, and they were recognized by antibodies against the FLAG epitope present on the σ-1 receptor construct. Hence, we are confident that the peripheral particles are σ-1 receptors. When we imaged complexes between ASICs and σ-1 receptors, the mean angle between pairs of bound σ-1 receptors was again close to 120°. These data argue strongly for a direct 1:1 binding between the σ-1 receptor and an ASIC subunit, meaning that the ASIC complex will bind a maximum of three σ-1 receptors.

The proportion of ASICs that were decorated by one and two σ-receptors was 11.4% and 1.3%, respectively. Only a minority (typically ~20%) of the ASIC-expressing cells were transfected with σ-1 receptor cDNA, so only this proportion of the ASICs would be exposed intracellularly to σ-1 receptors. Of these ASICs, the proportion decorated by one or two σ-1 receptors would therefore be ~57.0% and 6.5%, respectively, assuming that no ASIC/σ-1 receptor interaction occurred after cell lysis.

We found that the association between σ-1 receptors and ASICs was reduced by ~50% on treatment of the cells with the σ-1 receptor ligand haloperidol. However, this uncoupling did not lead to a change in the distribution of either protein between raft and non-raft phases of the membrane. Our observation that the σ-1 receptor is predominantly excluded from rafts differs from two previous reports that showed raft association of the receptor in MDA-MB-231 human breast cancer cells (17) and in endoplasmic reticulum-derived lipid droplets in NG108 cells (36). We speculate that the difference in behavior of the σ-1 receptor in these studies may be a result of the different cell lines used. The possibility remains that in these other cells, the action of σ-1 receptor ligands might affect the distribution of the receptor and its target channels within the plane of the membrane.

How might a reduction in coupling between the σ-1 receptor and ASIC1a bring about the observed reduction in ASIC1a-mediated membrane current (19)? The simplest possibility is that the binding of the σ-1 receptor to ASIC1a has a direct positive modulatory role, and that haloperidol brings about its functional effect by reducing this binding. However, this idea runs counter to previous findings that unliganded σ-1 receptors have a negative effect on channel current; for instance, σ-1 receptors increase the rate of inactivation of Kv1.4 and reduce the current at all voltages when the two proteins are coexpressed in *Xenopus* oocytes (4). An alternative possibility is that σ-1 receptors have an effect on the behavior of the ASIC channel akin to the interaction between G-protein-coupled receptors and G-proteins, where activation of the receptor is transmitted to the G-protein, but the affinity of the receptor for the G-protein falls.

If the effects of σ-receptors on the various ion channels involve similar direct interactions to the one described here, it will be revealing to see whether the 1:1 stoichiometry between σ-receptors and channel subunits is maintained. If so, one would expect the distribution of angles between pairs of bound σ-receptors and the tetrameric voltage-gated K^+, Na^+, and Ca^{2+} channels to have two peaks, at 90° and 180°. It should be possible to test this prediction using the type of analysis described here. We should also be able to use this approach to screen for regions involved in the interaction of the σ-1 receptor with its various ion channel targets.

We thank Nelson Barrera for helpful comments on the manuscript.

This work was supported by a grant from the Biotechnology and Biological Sciences Research Council (BB/D015545/1) to R.M.H. and J.M.E. M.B.J. was the recipient of a Parke Davis Exchange Fellowship in Biomedical Sciences.

REFERENCES

1. Martin, W. R., C. G. Eades, …, P. E. Gilbert. 1976. The effects of morphine- and nalorphine-like drugs in the nondependent and morphine-dependent chronic spinal dog. *J. Pharmacol. Exp. Ther.* 197:517–532.
2. Monnet, F. P. 2005. σ-1 Receptor as regulator of neuronal intracellular Ca^{2+}: clinical and therapeutic relevance. *Biol. Cell.* 97:873–883.
3. Hanner, M., F. F. Moebius, …, H. Glossmann. 1996. Purification, molecular cloning, and expression of the mammalian σ1-binding site. *Proc. Natl. Acad. Sci. USA.* 93:8072–8077.
4. Aydar, E., C. P. Palmer, …, M. B. Jackson. 2002. The σ receptor as a ligand-regulated auxiliary potassium channel subunit. *Neuron.* 34:399–410.
5. Hayashi, T., and T. P. Su. 2007. σ-1 Receptor chaperones at the ER-mitochondrion interface regulate Ca^{2+} signaling and cell survival. *Cell.* 131:596–610.
6. Kennedy, C., and G. Henderson. 1990. Inhibition of potassium currents by the σ receptor ligand (+)-3-(3-hydroxyphenyl)-N-(1-propyl)piperidine in sympathetic neurons of the mouse isolated hypogastric ganglion. *Neuroscience.* 35:725–733.
7. Wilke, R. A., R. P. Mehta, …, M. B. Jackson. 1999. σ Receptor photolabeling and σ receptor-mediated modulation of potassium channels in tumor cells. *J. Biol. Chem.* 274:18387–18392.
8. Zhang, H., and J. Cuevas. 2005. σ Receptor activation blocks potassium channels and depresses neuroexcitability in rat intracardiac neurons. *J. Pharmacol. Exp. Ther.* 313:1387–1396.
9. Johannessen, M., S. Ramachandran, …, M. B. Jackson. 2009. Voltage-gated sodium channel modulation by σ-receptors in cardiac myocytes and heterologous systems. *Am. J. Physiol. Cell Physiol.* 296:C1049–C1057.
10. Zhang, H., and J. Cuevas. 2002. σ Receptors inhibit high-voltage-activated calcium channels in rat sympathetic and parasympathetic neurons. *J. Neurophysiol.* 87:2867–2879.

11. Lysko, P. G., R. C. Gagnon, …, G. Feuerstein. 1992. Neuroprotective effects of SKF 10,047 in cultured rat cerebellar neurons and in gerbil global brain ischemia. *Stroke*. 23:414–419.
12. Ishiguro, H., T. Ohtsuki, …, T. Arinami. 1998. Association between polymorphisms in the type 1 σ receptor gene and schizophrenia. *Neurosci. Lett*. 257:45–48.
13. Fontanilla, D., M. Johannessen, …, A. E. Ruoho. 2009. The hallucinogen *N,N*-dimethyltryptamine (DMT) is an endogenous σ-1 receptor regulator. *Science*. 323:934–937.
14. Seth, P., M. E. Ganapathy, …, V. Ganapathy. 2001. Expression pattern of the type 1 σ receptor in the brain and identity of critical anionic amino acid residues in the ligand-binding domain of the receptor. *Biochim. Biophys. Acta*. 1540:59–67.
15. Pal, A., A. R. Hajipour, …, A. E. Ruoho. 2007. Identification of regions of the σ-1 receptor ligand binding site using a novel photoprobe. *Mol. Pharmacol*. 72:921–933.
16. Pal, A., U. B. Chu, …, A. E. Ruoho. 2008. Juxtaposition of the steroid binding domain-like I and II regions constitutes a ligand binding site in the σ-1 receptor. *J. Biol. Chem*. 283:19646–19656.
17. Palmer, C. P., R. Mahen, …, E. Aydar. 2007. σ-1 Receptors bind cholesterol and remodel lipid rafts in breast cancer cell lines. *Cancer Res*. 67:11166–11175.
18. Lupardus, P. J., R. A. Wilke, …, M. B. Jackson. 2000. Membrane-delimited coupling between σ receptors and K^+ channels in rat neurohypophysial terminals requires neither G-protein nor ATP. *J. Physiol*. 526:527–539.
19. Herrera, Y., C. Katnik, …, J. Cuevas. 2008. σ-1 Receptor modulation of acid-sensing ion channel a (ASIC1a) and ASIC1a-induced Ca^{2+} influx in rat cortical neurons. *J. Pharmacol. Exp. Ther*. 327:491–502.
20. Wemmie, J. A., M. P. Price, and M. J. Welsh. 2006. Acid-sensing ion channels: advances, questions and therapeutic opportunities. *Trends Neurosci*. 29:578–586.
21. Jasti, J., H. Furukawa, …, E. Gouaux. 2007. Structure of acid-sensing ion channel 1 at 1.9 A resolution and low pH. *Nature*. 449:316–323.
22. Carnally, S. M., H. S. Dev, …, J. M. Edwardson. 2008. Direct visualization of the trimeric structure of the ASIC1a channel, using AFM imaging. *Biochem. Biophys. Res. Commun*. 372:752–755.
23. Benson, C. J., J. Xie, …, P. M. Snyder. 2002. Heteromultimers of DEG/ENaC subunits form H^+-gated channels in mouse sensory neurons. *Proc. Natl. Acad. Sci. USA*. 99:2338–2343.
24. Yermolaieva, O., A. S. Leonard, …, M. J. Welsh. 2004. Extracellular acidosis increases neuronal cell calcium by activating acid-sensing ion channel 1a. *Proc. Natl. Acad. Sci. USA*. 101:6752–6757.
25. Barrera, N. P., S. J. Ormond, …, J. M. Edwardson. 2005. AFM imaging demonstrates that P2X2 receptors are trimers but that P2X6 receptor subunits do not oligomerize. *J. Biol. Chem*. 280:10759–10765.
26. Barrera, N. P., P. Herbert, …, J. M. Edwardson. 2005. Atomic force microscopy reveals the stoichiometry and subunit arrangement of 5-HT_3 receptors. *Proc. Natl. Acad. Sci. USA*. 102:12595–12600.
27. Barrera, N. P., J. Betts, …, J. M. Edwardson. 2008. Atomic force microscopy reveals the stoichiometry and subunit arrangement of the $\alpha_4\beta_3\delta$ $GABA_A$ receptor. *Mol. Pharmacol*. 73:960–967.
28. Barrera, N. P., Y. Shaifta, …, J. M. Edwardson. 2007. AFM imaging reveals the tetrameric structure of the TRPC1 channel. *Biochem. Biophys. Res. Commun*. 358:1086–1090.
29. Barrera, N. P., H. Ge, …, J. M. Edwardson. 2008. Automated analysis of the architecture of receptors, imaged by atomic force microscopy. *Micron*. 39:101–110.
30. Meltzer, R. H., N. Kapoor, …, D. J. Benos. 2007. Heteromeric assembly of acid-sensitive ion channel and epithelial sodium channel subunits. *J. Biol. Chem*. 282:25548–25559.
31. Neaves, K. J., L. P. Cooper, …, R. M. Henderson. 2009. Atomic force microscopy of the EcoKI type I DNA restriction enzyme bound to DNA shows enzyme dimerization and DNA looping. *Nucleic Acids Res*. 37:2053–2063.
32. Martens, J. R., N. Sakamoto, …, M. M. Tamkun. 2001. Isoform-specific localization of voltage-gated K^+ channels to distinct lipid raft populations. Targeting of Kv1.5 to caveolae. *J. Biol. Chem*. 276:8409–8414.
33. Wong, W., and L. C. Schlichter. 2004. Differential recruitment of Kv1.4 and Kv4.2 to lipid rafts by PSD-95. *J. Biol. Chem*. 279:444–452.
34. Schuck, S., M. Honsho, …, K. Simons. 2003. Resistance of cell membranes to different detergents. *Proc. Natl. Acad. Sci. USA*. 100:5795–5800.
35. Schneider, S. W., J. Lärmer, …, H. Oberleithner. 1998. Molecular weights of individual proteins correlate with molecular volumes measured by atomic force microscopy. *Pflugers Arch*. 435:362–367.
36. Hayashi, T., and T.-P. Su. 2003. σ-1 Receptors ($\sigma_{(1)}$ binding sites) form raft-like microdomains and target lipid droplets on the endoplasmic reticulum: roles in endoplasmic reticulum lipid compartmentalization and export. *J. Pharmacol. Exp. Ther*. 306:718–725.